The paper was presented at the Eleventh Meeting “New Trends in Fatigue and Fracture” (NT2F11) Polignano a Mare, Italy, 3–6 July, 2011

George Wardeh, Elhem Ghorbel

FRACTURE BEHAVIOUR OF FROST DAMAGED CONCRETE
LOM BETONA OŠTEĆENOG MRŽNJENJEM

Originalni naučni rad / Original scientific paper
UDK /UDC: 620.1:691.32
Rad primljen / Paper received: 21.01.2012

Adresa autora / Author's address:
University of Cergy-Pontoise, Neuville Sur Oise, Cergy-Pontoise Cedex, France, George.Wardeh@u-cergy.fr

Keywords
- frost action
- fracture parameters
- crack propagation

Ključne reči
- dejstvo zamrzavanja
- parametri loma
- rast prsline

Abstract

The aim of this work is to characterize the toughness of frost damaged normal vibrated concrete. From force-deflection and force-crack opening curves, obtained by means of three-point bending tests performed on notched specimens, toughness parameters are evaluated as a function of freezing-thawing cycle numbers. The results show that the stress intensity factor, K_{IC}, and the flexural tensile strength, σ_{ft}, decrease while the critical crack mouth opening displacement $CMOD_c$, increases. The variation of these parameters is correlated to the degree of concrete damage characterized by the relative variation of flexural strength and an analytical model of crack propagation is used for the interpretation of results.

Izvod

Cilj ovog rada je u karakterizaciji žilavosti klasično vibriranog betona, oštećenog mržnjenjem. Sa dijagrama sila-ugib i sila-otvaranje prsline, dobijenih ispitivanjem savijanjem u tri tačke, koje je izvedeno sa zarezanim epruvetama, parametri žilavosti su sračunati kao funkcija broja ciklusa zamrzavanja-odmrzavanja. Rezultati pokazuju da faktor intenziteta napona, K_{IC}, i savojna zatezna čvrstoća, σ_{ft}, opadaju, a kritično otvaranje usta prsline, $CMOD_c$, opada. Primenjena je korelacija varijacije ovih parametara do stepena oštećenja betona, koje je okarakterisano relativnom varijacijom savojne čvrstoće, a takođe je primenjen i analitički model rasta prsline za tumačenje dobijenih rezultata.

INTRODUCTION

Concrete is a porous material which, when water saturated, is vulnerable by frost action. At subzero temperature, water is gradually transformed into ice and the phenomenon is accompanied by a volumetric expansion of about 9% and a hydraulic pressure builds up, /1, 2/. This can be dissipated by water flow within the unfrozen porous network to find an outlet, and its magnitude depends on the permeability of the media. The generated pressure may be harmful and induce concrete cracking when expelled water cannot move easily to an empty air void. The crystallization pressure is also added to this hydraulic pressure, which is related to the crystal growth within frozen pores, /3/.

Repeated freezing-thawing cycles alter the physical and mechanical properties of concrete, such as the elasticity modulus, compressive and flexural strength and permeability. However, we do not have much information on the evolution of the stress intensity factor, K_{IC}, the fracture energy G_F and the critical mouth opening displacement $CMOD_c$, which are fundamental parameters required for most models of damage or fracture mechanics of concrete.

In this study, the variation of these parameters during freeze-thaw cycles is studied using the results of three-point bending tests performed on notched beams and two-parameter model, /4/ ($CMOD_c$ and K_{IC}) . The model requires prior knowledge of real crack length corresponding to the maximum load, thus an analytical model is proposed to evaluate it.

MATERIALS AND EXPERIMENTAL PROGRAMME

Materials

A CEM I CALCIA 52.5N CE CP2 NF Cement, 0/4 mm siliceous, rolled sand with a density of 2.55 and siliceous semi-crushed gravel 4/20 mm with a density of 2.51 were used. The mixed material is a traditionally vibrated concrete of S4 workability class where the slump with the Abrams’s cone is 180 ± 20 mm and XF2 class of environmental exposure according to EN 206-1, /5/. In order to achieve concrete workability, a Cimfluid 2002 based on modified polycarboxylate superplasticizer, SP, is also employed. Table 1 recapitulates the composition and the mix proportion of the prepared concrete and its properties in fresh state.

Table 1. Mix proportions of the used concrete.
Tabela 1. Odnosi mešanja upotrebljenog betona

Cement (kg/m^3)	Gravel (kg/m^3)	Sand (kg/m^3)	Water (kg/m^3)	SP (kg/m^3)	Density (kg/m^3)	Air content %
350	1065	720	164	1.89	2200	1.5

EXPERIMENTAL METHODS

Cylindrical 16 × 32 cm^2 specimens and 8 × 15 × 70 cm^3 prismatic beams with notches of 5 cm are prepared in order to follow the strength and the fracture parameters' evolution during the freezing–thawing test. 24 h after moulding all specimens are preserved in water at room temperature for 28 days before submitting them to the freezing–thawing test. For this test, cycles of 12 h duration are imposed according to the Rilem recommendations, /6-8/. The freezing/thawing cycles are carried out without water contribution, but each specimen is covered by a plastic film to avoid evaporation.

Starting from +10°C the temperature is lowered in 3 h with a cooling rate of 10°C/h down to –20°C, and kept constant during 3 h at this temperature. Then it is increased during 2 h to +10°C with a warming rate of 15°C/h and kept constant during 4 h. These steps are programmed in order to stabilize the temperatures and to allow the liquid transfers to occur. So the basic loop includes two cycles per day.

The evolution of the temperature during one cycle is illustrated in Fig. 1. In this figure, we can observe that the actual temperature is close to that of the reference as well as a good homogeneity of the thermal distribution within a cylinder 16 × 32 cm instrumented with five thermocouples.

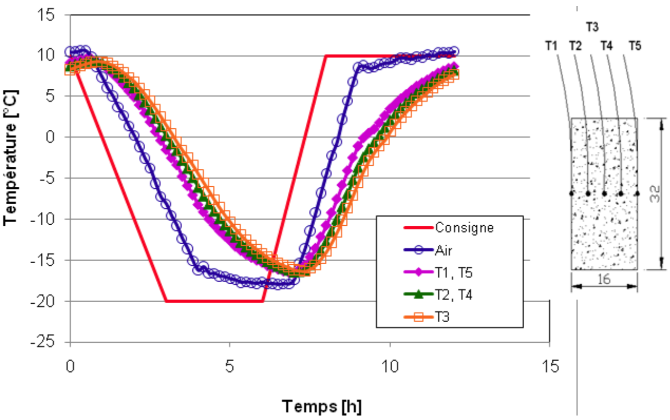

Figure 1. Profile of freezing thawing cycles.
Slika 1. Profil ciklusa zamrzavanja i topljenja

PROPERTIES OF CONCRETE IN HARDENED STATE

The material's ability to resist cracking is characterized by its specific fracture energy noted G_F dissipated during crack opening. The crack, which is usually assumed to grow in mode I, becomes unstable when the stress intensity factor reaches a critical value, denoted by K_{IC}, /4/. Within the framework of linear elastic fracture mechanics, one can establish relations between fracture energy and stress intensity factor of metals or brittle material such as glass and ceramics. However, for materials due to softening behaviour such as concrete, experience shows that these two parameters are not intrinsic and depend on the size and geometry of the studied specimen, /9-11/. This dependence is due to the existence of a microcracked zone of considerable length named Fracture Process Zone 'FPZ' in which stress transfer is still active and depends on the crack opening, /12, 13/. Thus, G_F and K_{IC} should be completed by other parameters which are respectively, the length of the FPZ and the critical crack opening displacement $CMOD_c$.

From a force-displacement curve, recorded during 3 bending tests, fracture energy, G_F, can be calculated by the equation, /14/:

$$G_F = \frac{W_0 + (m_1 + 2m_2) g \delta_0}{A_{lig}} \tag{1}$$

Where W_0 is the area below the force-displacement curve, m_1 –weight of the beam between the supports, m_2 –weight of the loading arrangement not attached to the machine, g –acceleration due to gravity, δ_0 –deformation of the final failure of the specimen, and A_{lig} –area of ligament defined as the projection of the fracture zone on a plane perpendicular to the median line of the beam.

Stress intensity factor K_{IC} and crack mouth opening displacement may be calculated by means of Fig. 2 and the following relations, /15/:

$$K_{IC} = \sigma_{NC} \sqrt{\pi a_c} \cdot f_1(\alpha) \tag{2}$$

$$CMOD_c = \frac{4\sigma_{NC} \cdot \alpha_C}{E} f_2(\alpha) f_3(\alpha,\beta) \tag{3}$$

with $\sigma_{NC} = \dfrac{3F \cdot S}{2bd^2}$, $\alpha = \dfrac{a_c + d_0}{d + d_0}$ and $\beta = \dfrac{a_c}{a_0}$.

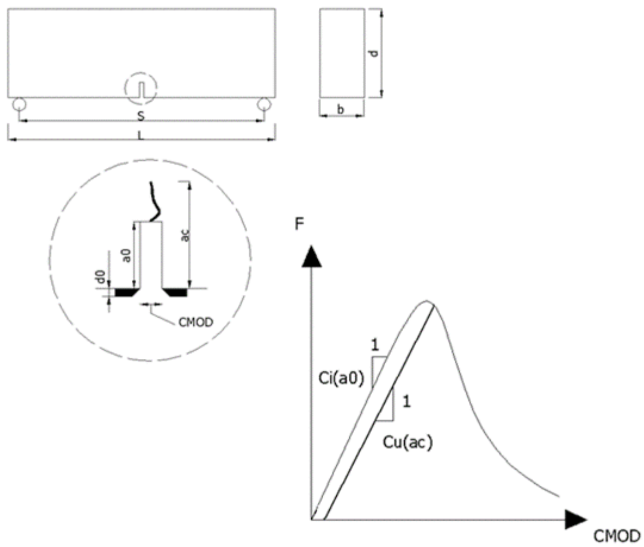

Figure 2. Determination of fracture parameters of concrete: a) geometrically characteristic values, b) typical F-CMOD curve.
Slika 2. Određivanje parametara mehanike loma betona: a) geometrijske karakteristike, b) tipična kriva F-CMOD

Functions f_1, f_2, f_3 are given by following relations:

$$f_1(\alpha) = \frac{1.83 - 1.85\alpha + 4.76\alpha^2 - 5.3\alpha^3 + 2.51\alpha^4}{(1+2\alpha)(1-\alpha)^{3/2}} \tag{4}$$

$$f_2(\alpha) = 0.65 - 1.88\alpha + 3.02\alpha^2 - 2.69\alpha^3 + \frac{0.68}{(1-\alpha)^2} \tag{5}$$

$$f_3(\alpha,\beta) = \sqrt{(1-\beta)^2 + (1.081 - 1.149\alpha)(\beta - \beta^2)} \tag{6}$$

In the previous equations, the critical crack length is given by equation:

$$a_c = a_0 \frac{C_u f_2(\alpha_0)}{C_i f_2(\alpha)}, \quad \alpha_0 = \frac{a_0}{d} \tag{7}$$

For the studied concrete, the mechanical properties and fracture parameters are given in the following table.

Table 2. Mechanical properties and fracture parameters of the studied concrete.
Tabela 2. Mehaničke osobine i parametri loma ispitanog betona

Elastic modulus (GPa)	Compressive strength (MPa)	Flexural strength (MPa)	G_F (N/mm)	K_{IC} (MPa·Mm$^{0.5}$)	CMOD$_c$ (mm)
35	30	5.3	0.2	690	0.06

EVOLUTION OF DEGRADATIONS DURING TESTING

In order to appreciate frost damage, surfaces of cylindrical and prismatic specimens are studied after every 30 freezing–thawing cycles. All the cylinders had a single model of cracking for which cracks are oriented in axial and radial directions. These typical modes of cracking are due to the hydrostatic nature of pore pressure build-up during the freezing-thawing cycles. Moreover, this phenomenon is often accompanied by a surface scaling when the material is fully saturated, /16/. For prismatic specimens, cracks are randomly oriented (Fig. 3).

a) 

b) 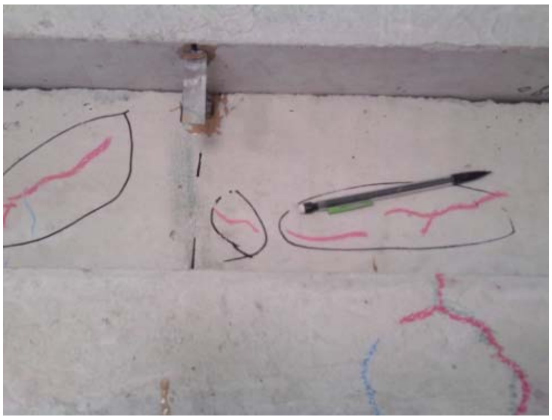

Figure 3. Frost damages specimens after 240 freezing-thawing cycles, a) cylindrical specimen after 240 cycles, b) prismatic specimen after 240 cycles
Slika 3. Oštećenja usled zamrzavanja nakon 240 ciklusa zamrzavanja-topljenja, a) cilindrični uzorak nakon 240 ciklusa, b) prizmatični uzorak posle 240 ciklusa

In order to quantify the effect of repeated freezing-thawing cycles on the performance of the studied material, the relative variation of each characteristic (*damage factor*) is evaluated. This variation can be defined by the following expression:

$$D_g^{\Im} = \frac{\Im - \bar{\Im}}{\Im} \tag{8}$$

where $\Im$ is the property related to the non-damaged material, $\bar{\Im}$ the same property after N freezing-thawing cycles and $D_g^{\Im}$ the damage factor.

Figure 4 shows the evolution of the damage factor related to the elastic modulus, the compressive strength and the flexural strength with the number of cycles. In this figure one can observe that the variation in flexural strength is more pronounced than other mechanical properties. After 100 cycles, the damage factor is about 0.4 and it is equal to 0.65 at the end of the 210th cycle.

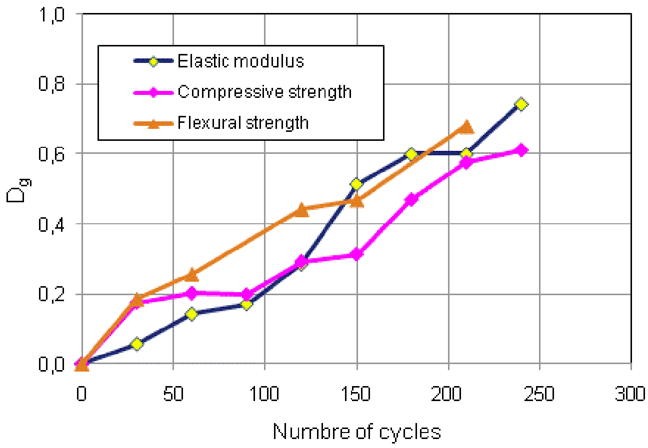

Figure 4. Damage factors' evolution with freezing-thawing cycles.
Slika 4. Razvoj faktora oštećenja sa ciklusima zamrzavanja-topljenja

The following figure presents force-CMOD curves as a function of cycle number. The curves highlight the following observations: a decrease in stiffness during the cycles resulting in a reduction of the maximal load, an increase of the crack opening, and a significant change in the post-peak behaviour. This behaviour, similar to that of concrete at high temperatures, is due to the fracture energy increase despite decrease in elastic modulus and tensile strength, /17/.

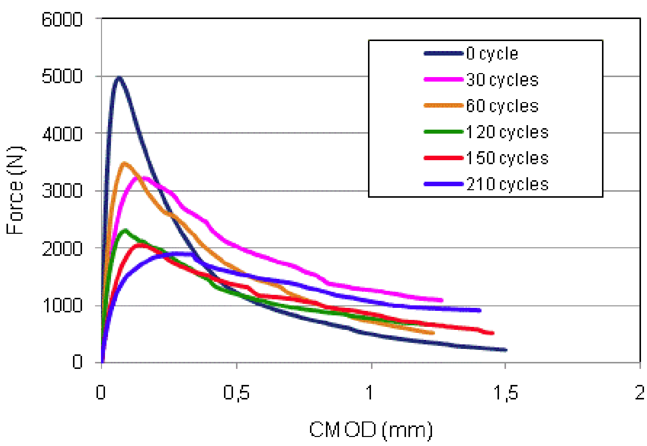

Figure 5. Force-CMOD curves as a function of cycle number.
Slika 5. Opterećenje-CMOD krive u funkciji broja ciklusa

CRACK PROPAGATION RESISTANCE

The calculation of stress intensity factor requires the exact length of the crack, a_c, by performing cycles of loading-unloading as it is previously presented. Although the realisation of these cycles is possible on the undamaged specimen, it is almost impossible on damaged ones. Thus we choose to calculate analytically, based on the cracked hinge model, /18/. According to this model, the failure of a beam loaded in three point bending is studied assuming the development of a single fictitious crack in a narrow zone, the hinge, while outside it the material retains its elastic behaviour, Fig. 6.

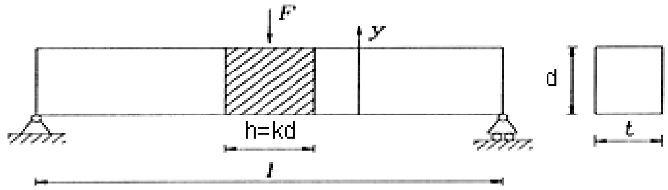

Figure 6. Beam in three-point bending: the hatched area represents the fractured hinge.
Slika 6. Nosač pri savijanju u tri tačke: šrafirana površina predstavlja zglobni lom

The crack develops in the midsection of the beam when the tensile stress reaches its ultimate value, σ_u, and then spreads over a layer of thickness h. The crack progresses while increasing the load where the material is softened by cohesive forces in the fracture process zone, /12, 13/. When the crack opening reaches the critical value, w_c, the section reaches the third stage during which the crack is no longer able to transfer constraints, Fig. 7.

In the cracked zone the cracking process is described by a softening constitutive law which relates the normal tensile stress, σ, to the crack opening, w by the relation:

$$\frac{\sigma}{\sigma_u}=1-\left(\frac{w}{w_c}\right)^n,\ 0<n\leq 1 \qquad (9)$$

With w_c, the critical crack opening when the stress reaches zero.

The complete flexural behaviour during the three phases is described below:

Phase 1:

Instead of the bending moment, M and the real rotation ϕ, it is more convenient to introduce the non-dimensional bending moment, μ, and the corresponding dimensionless rotation θ defined as follows:

$$\mu=\frac{6M}{bd^2\sigma_u} \qquad (10)$$

$$\theta=\frac{dE}{h\sigma_u}\phi \qquad (11)$$

With E: the elasticity modulus of the material. This leads to a simple linear relationship between μ and θ.

$$\mu(\theta)=\theta \qquad (12)$$

At the end of the elastic phase we have: $\mu=\theta=1$.

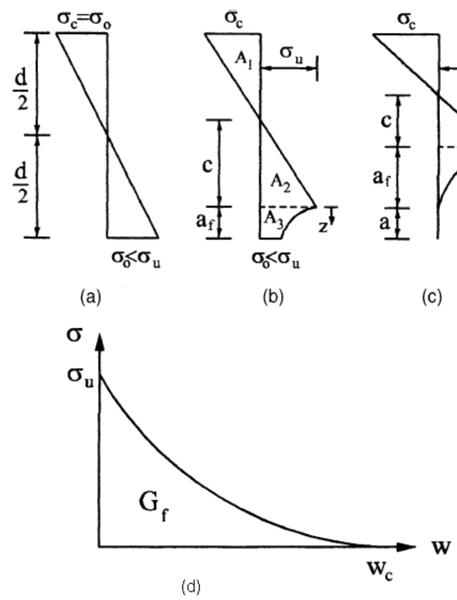

Figure 7. Stress distributions in different phases. (a) Phase I–elastic stress distribution, (b) Phase II–with a fictitious crack length a_f, (c) with a fictitious crack length a_f and a real crack length a, and (d) σ-w relation.
Slika 7. Raspodele napona u različitim fazama. (a) Faza I–raspodela elastičnog napona. (b) Faza II–sa fiktivnom prslinom dužine a_f, (c) sa fiktivnom prslinom dužine a_f i realnom prslinom dužine a, i (d) σ-w relacija

Phase 2:

Based on Figs. 7b and d, static equilibrium of the forces leads to the following relation between μ and θ:

$$\mu=\frac{1}{2\theta^2}\left[\begin{array}{c}\left\{2\theta-\left(1+\frac{w_0}{Bw_c}-\left(\frac{w_0}{w_c}\right)^n\right)\right\}^{\beta}+1+\\ \frac{3}{m+1}\left(\frac{w_0}{w_c}-\left(\frac{w_0}{w_c}\right)^n\right)\left(m+1-\left(\frac{w_0}{w_c}\right)^n\right)\left(1+\frac{\bar{z}}{c}\right)\end{array}\right] \qquad (13)$$

With w_0 the crack opening at the bottom edge, and

$$\frac{\bar{z}}{c}=\frac{m+1}{m+2}\left(\frac{\frac{m}{2}+1-\left(\frac{w_0}{w_c}\right)^n}{m+1-\left(\frac{w_0}{w_c}\right)^n}\right)\left(\frac{w_0}{Bw_c}-\left(\frac{w_0}{w_c}\right)^n\right) \qquad (14)$$

B describes material brittleness and is given by:

$$B=\frac{n}{n+1}\frac{\sigma_u^2 h}{EG_F},\ 0\leq B\leq 1 \qquad (15)$$

And finally m is expressed as:

$$m=\frac{2n-B(n+1)}{2-B(n+1)} \qquad (16)$$

Rotation during this phase is expressed by the equation:

$$w_0-Bw_c\left(\frac{w_0}{w_c}\right)^n=2\phi\cdot a_f \qquad (17)$$

The end of phase 2 is reached when the crack opening at the bottom fibre, w_0, is equal to the critical crack opening. The dimensionless rotation which marks this state is given by:

$$\theta_c = \frac{1}{2B} + \frac{1}{2}\sqrt{1 + \frac{2m}{m+1}\frac{1-B}{B}} \tag{18}$$

The procedure of analysis is to seek the solution of Eq.(13) by an iterative method, using Excel's solver, for example, and then to calculate the rotation by means of Eq.(17).

– Phase 3:

In phase 3, the real crack length is termed as a, and we have the following relations:

$$\frac{a_f}{d} = \frac{1-B}{B}\frac{1}{\theta} \tag{19}$$

$$\frac{a}{d} = 1 - \frac{\theta_c}{\theta} \tag{20}$$

$$\mu = \mu_c\left(\frac{\theta_c}{\theta}\right)^2 \tag{21}$$

With $\mu_c = \dfrac{\dfrac{4n}{n+1}\sqrt{\dfrac{n}{n+1}2B} + \dfrac{6n^2B}{(n+1)(2n+1)} + \dfrac{3n}{n+2}}{\left(\sqrt{\dfrac{2Bn}{n+1}} + 1\right)^2}$

For all phases the dimensionless displacement is given by the relation:

$$\theta_t = \theta + (\gamma - 1)\mu \tag{22}$$

Where $\gamma = \dfrac{F\lambda}{3k}$, $F = 1 + \dfrac{2.85}{\lambda^2} - \dfrac{0.84}{\lambda^3}$ and $\lambda = \dfrac{l}{d}$.

For the non-frost damaged beam, the following parameters are found by a calibration between the real force-CMOD curve and the simulated one: G = 0.1 N/mm and n = 0.5. Then the crack length corresponding to peak load obtained by this analytical model is compared to that obtained by the finite element method and a perfect agreement is found between the two methods.

The analytical model is used to calculate the real crack length of each frost damaged beam. To find this length, the parameters of Eq.(13) are calibrated to find the curve that is most closest to the experimental curve, and then the stress intensity factor and critical crack opening are calculated respectively, using Eqs.(2) and (3).

Figure 8 depicts the variation of K_{IC} as a function of the damage factor related to the change in flexural strength, where one can observe that K_{IC} varies linearly with the degree of damage. With regards to the critical crack opening, it is found that it varies a little at the beginning of the freezing/thawing test and then increases significantly when the number of cycles becomes important.

CONCLUSION

This study concerns the variation of fracture properties of concrete exposed to freeze-thaw cycles. When the number of cycles increases, the modulus of elasticity, compressive and flexural strength decrease and the fracture behaviour of the material becomes more ductile. The stress intensity factor decreases with cycles and a linear correlation is found between this reduction and increased damage factor related to the process of frost damage.

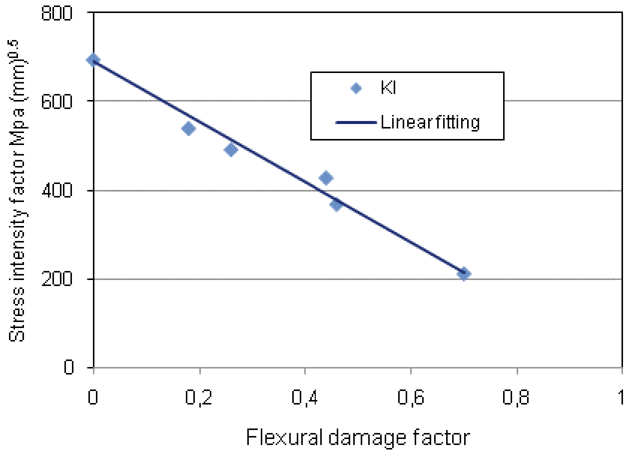

Figure 8. Relationship between stress intensity factor and flexural damage factor.

Slika 8. Veza između faktora intenziteta napona i faktora oštećenja pri savijanju

REFERENCES

1. Powers, T.C., *The air requirement of frost-resistant concrete*, Proc. Highway Res. Board. 1949.
2. Powers, T.C., Helmuth, R.A., *Theory of volume changes in hardened Portland cement paste during freezing*, Proc. Highway Res. Board, 1953.
3. Scherer, G.W., *Crystallization in pores*, Cement and Concrete Research, 1999, 29(8): pp.1347-1358.
4. Shah, S.P., Swartz, S.E., Fracture mechanics of concrete: applications of fracture mechanics to concrete, rock and other quasi-brittle materials, 1995, New York: Wiley, p.552.
5. AFNOR, NF EN 206-1. L'Association française de Normalisation, 2004.
6. AFNOR, NF P18-424. L'Association française de Normalisation, 2004.
7. AFNOR, NF P18-425. L'Association française de Normalisation, 2004.
8. Setzer, M.J., et al., *CIF-Test-Capillary suction, internal damage and freeze thaw test*, Materials and Structures, 2001, 34(9): pp.515-525.
9. Rosselló, C., Elices, M., *Fracture of model concrete: 1. Types of fracture and crack path*, Cement and Concrete Research, 2004, 34(8): pp.1441-1450.
10. Issa, M., et al., *Size effects in concrete fracture: Part I, experimental setup and observations*, International Journal of Fracture, 2000, 102(1): pp.1-24.
11. Kwon, S.H., Zhao, Z., Shah, S.P., *Effect of specimen size on fracture energy and softening curve of concrete: Part II. Inverse analysis and softening curve*, Cement and Concrete Research, 2008, 38(8-9): pp.1061-1069.
12. Hillerborg, A., Modéer, M., Petersson, P.-E., *Analysis of crack formation and crack growth in concrete by means of fracture mechanics and finite elements*, Cement and Concrete Research, 1976, 6(6): pp.773-781.
13. Hillerborg, A., *The theoretical basis of a method to determine the fracture energy G_F of concrete*, Materials and Structures, 1985, 18(4): pp.291-296.

14. 50-FMC Draft Recommendation, *Determination of the fracture energy of mortar and concrete by means of three-point bend tests on notched beams*, Materials and Structures/ Matériaux et Constructions, 1985, 18(4): pp.287-290.
15. Lee, M.K., Barr, B.I.G., *Strength and fracture properties of industrially prepared steel fibre reinforced concrete*, Cement and Concrete Composites, 2003, 25(3): pp.321-332.
16. Wardeh, G., Mohamed, M.A.S., Ghorbel, E., *Analysis of concrete internal deterioration due to frost action*, Journal of Building Physics, 2010, doi:10.1177/1744259110370854.
17. Menou, A., et al., *Residual fracture energy of cement paste, mortar and concrete subject to high temperature*, Theoretical and Applied Fracture Mechanics, 2006, 45(1): pp.64-71.
18. Sundara Raja Iyengar, K.T., Raviraj, S., Jayaram, T.N., *Analysis of crack propagation in strain-softening beams*, Engineering Fracture Mechanics, 2002, 69(6): pp.761-778.